The Fifth International Workshop on Micro and Nanotechnology for Power Generation and Energy Conversion Applications
PowerMEMS 2005
Nov. 28-30, 2005
Takeda Hall, The University of Tokyo, Tokyo, Japan

Microball-Bearing-Supported Electrostatic Micromachines with Polymer Dielectric Films for Electromechanical Power Conversion

A. Modafe[1], N. Ghalichechian[1], A. Frey[1], J. H. Lang[2], and R. Ghodssi[1]
[1]MEMS Sensors and Actuators Lab (MSAL)
Department of Electrical and Computer Engineering, The Institute for Systems Research
University of Maryland, College Park, MD 20742, USA
[2]Department of Electrical Engineering and Computer Science
Massachusetts Institute of Technology, Cambridge, MA 02139, USA

Abstract

We report our research activities toward the development of a rotary electrostatic micromotor/microgenerator with a microball-bearing support mechanism and benzocyclobutene (BCB) low-k polymer insulating layers. The primary applications of this device are high-speed micro pumping and micro power generation. In this paper, we present the basic design of the rotary micromachine, which is based on our recent work on a bottom-drive, linear, variable-capacitance micromotor (B-LVCM). The design and fabrication of the B-LVCM are reviewed and characterization of the motor capacitance and force in six-phase mode is presented for the first time. The B-LVCM consists of a silicon stator, a silicon slider, and four stainless-steel microballs. The operation of the B-LVCM in three-phase mode was verified by applying square-wave voltages and characterizing the slider motion. The aligning force profile of a six-phase B-LVCM was extracted from simulated and measured capacitances of all six phases. The linear micromotor is used as a platform for developing the rotary micromotor/ microgenerator supported on microball bearing.

Keywords: Microball Bearings, Benzocyclobutene Polymers, Variable-Capacitance Micromachine, Micromotor, Microgenerator

1 INTRODUCTION

Reliability and efficiency of power microelectromechanical systems (Power MEMS), such as micromotors and microgenerators have yet to reach their macroscale counterparts. In recent years, the demand for higher power density in sources of power for microsystems and portable electronics has pushed the standards to higher levels. In an effort to address this need, we have developed key enabling technologies for reliable and efficient electrostatic micromachines.

The first demonstration of such devices is a bottom-drive, linear, variable-capacitance micromotor (B-LVCM) [1] that integrates microball bearings in silicon [2] and thick low-dielectric-constant (low-k) benzocyclobutene (BCB) polymers [3]. The B-LVCM has been designed and fabricated based on our previous work on characterization and modeling of microball bearings [4, 5] and process integration of BCB polymers with silicon micromachining [6-8].

The B-LVCM is a long-range, high-speed, linear micropositioner that combines the characteristics of microball bearings (e.g. robustness, stability, and low friction and wear) with those of BCB polymer insulating layers (e.g. low electrical loss and residual stress) in a microelectromechanical device. Furthermore, it provides a technology platform to develop reliable, efficient rotary electrostatic micromotor/microgenerator.

In this paper, we present the latest results of our work on the B-LVCM and a basic design for a bottom-drive, rotary, variable-capacitance micromachine (B-RVCM). When operating in generator mode, the B-RVCM can supply power to a variety of microsystems and potable devices. The B-RVCM can also be used as a micromotor for applications such as micropumping, microassembly, micropropulsion, and microactuation.

2 LINEAR MICROMOTOR DESIGN

The B-LVCM consists of two silicon plates, stator and slider, and four stainless-steel microballs (Figure 1a). The slider is free to move and supported on the microballs (285 μm in diameter) housed in 290-μm wide parallel trenches etched in both silicon plates. The depths of these trenches define the air gap. The housings on each side of the stator active area consist of two separate trenches to prevent jamming and collision of the microballs. The active area

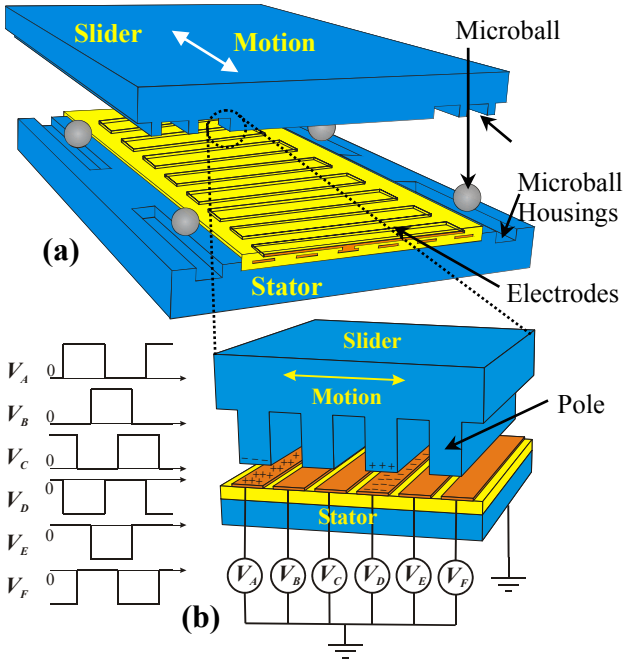

Figure 1. (a) Schematic 3D view of the six-phase, bottom-drive, linear, variable-capacitance micromotor, and (b) principle of operation and square-wave excitation.

consists of a stack of three BCB layers for insulation and passivation, and two metal layers for interconnects and electrodes. Each interconnect line connects every sixth electrodes to form a six-phase motor. Contrary to the stator, the trenches on the slider are continuous so that the maximum range of motion is achieved. Table 1 shows the design parameters for three different B-LVCM devices.

When the excitation voltage is applied to stator electrodes, image charges are induced on the slider poles (Figure 1b). The resulted electrostatic force aligns the active electrodes and poles, resulting in slider motion. The electrode to pole ratio is 6:4 where proper sequence of electrode excitation causes slider to move continuously. The aligning force generated by each phase can be written as

$$F_{ph} = \frac{1}{2} V_{ph}^2 \frac{\partial C_{ph}}{\partial x} \qquad (1)$$

where V_{ph} is the amplitude of the excitation voltage, C_{ph} is the B-LVCM capacitance per phase, and x is the position of the slider. Table 2 shows the estimated maximum aligning force for the three B-LVCM designs, assuming a minimum capacitance of zero and a linear profile for the spatial gradient of the capacitance. The maximum capacitance was numerically calculated using FEMLAB.

Since the B-LVCM is a synchronous machine, assuming a 50 % duty cycle for the excitation waveforms, the slider speed in steady-state continuous motion can be written as

$$u_{ave} = 2Wf_s \qquad (2)$$

Table 1. Three different designs of the B-LVCM.

Device	Air Gap (µm)	Electrode Width/Pitch (µm)	Pole Width/Pitch (µm)	Active Area (mm^2)
D1	5	30/40	30/60	50.25
D2	10	90/120	90/180	49.95
D3	20	180/240	180/360	49.50

Table 2. Estimated force and speed of the B-LVCM.

Device	Maximum Aligning Force at 100 V (mN)		Average Slider Speed (mm/s)		
	Per Phase	Six Phase	10 Hz	20 Hz	50 Hz
D1	1.61	4.82	0.6	1.2	3.0
D2	0.31	0.93	1.8	3.6	9.0
D3	0.08	0.23	3.6	7.2	18.0

where W is the electrode/pole width and f_s is the frequency of the stator excitation. The estimated average slider speed is also shown in Table 2.

3 LINEAR MICROMOTOR FABRICATION

As shown in Figure 2, fabrication of the stator starts with developing an isolated island of BCB based on a technique called "Embedded BCB in Silicon (EBiS)" process reported in our previous work [8]. The EBiS island forms the underlying insulating layer for the active area, where a BCB interlayer dielectric (ILD), two metal layers for phase interconnects and electrodes, and a BCB passivation layer are stacked. Finally, the microball housings are etched in the stator using deep reactive ion etching (DRIE). A fabricated stator is shown in Figure 3a.

The active area on the slider consists of parallel silicon poles etched into the silicon substrate together with the microball housings using DRIE (Figure 3b).

4 LINEAR MICROMOTOR CHARACTERIZATION

The DC and AC (in three-phase mode) operation of the B-LVCM was reported in [1] where an average linear speed of the slider up to 3.56 mm/s at 100 V, 20 Hz was achieved with some irregularities in slider motion. The measured speed is close to the predicted average speed, 3.6 mm/s as shown in Table 2. The operation of the motor in six phase mode is expected to provide a smoother motion.

Figure 4 shows the capacitance profile of all six phases versus slider position for device D2 with an estimated air gap of 19.2 µm. The total aligning force profiles calculated from the capacitance profiles (after a sine-squared curve fit and assuming a 100-V DC excitation voltage) are shown in Figure 5. There is a good agreement between the simulation and measurement average force. The discrepancy between these data and Table 2 is due to the difference between

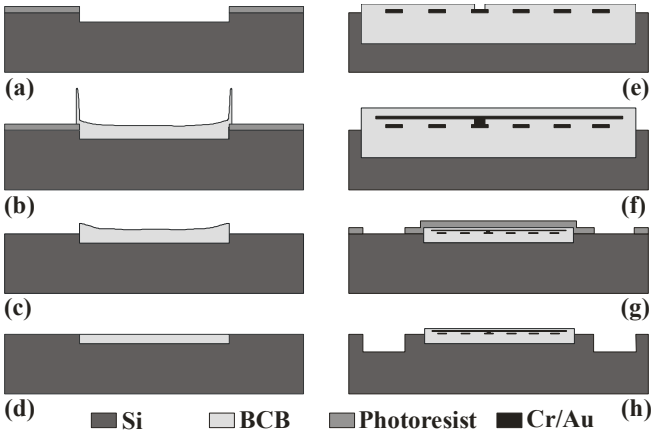

Fig. 2. Major process steps for fabrication of the B-LVCM stator: (a) etch Si pit with DRIE, (b) spin-cast and pattern photo-BCB, (c) lift off BCB ridges, (d) planarize EBiS island with CMP, (e) fabricate Cr/Au interconnects and pattern photo-BCB to open vias, (f) fabricate Cr/Au electrodes and pattern photo-BCB passivation layer, (g) and (h) etch trenches with DRIE.

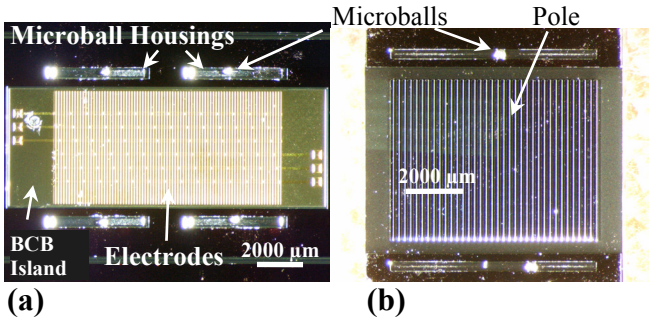

Figure 3. Optical micrograph of (a) a fabricated stator and (b) a DRIE-fabricated slider.

designed and fabricated air gap. The difference in profile, however, can be mainly associated with the non-uniformity of trench depth on the slider and defects in fabrication of the stator electrodes.

5 ROTARY MICROMACHINE DESIGN

The linear micromotor has been used as a platform for developing the rotary micromotor/microgenerator (Figure 6). This micromachine is first developed as a micromotor and then as a microgenerator. An array of radial electrodes grouped into six phases is designed on the stator active area. Similarly, an array of radial salient poles is arranged on the rotor such that the test-pads on the stator are easily accessible. Different geometries have been designed for developing micromachines that will exhibit desired electromechanical characteristics (speed, torque, and power). Electrode and pole geometries of the machine have been optimized using 3D finite element analysis (FEA) and

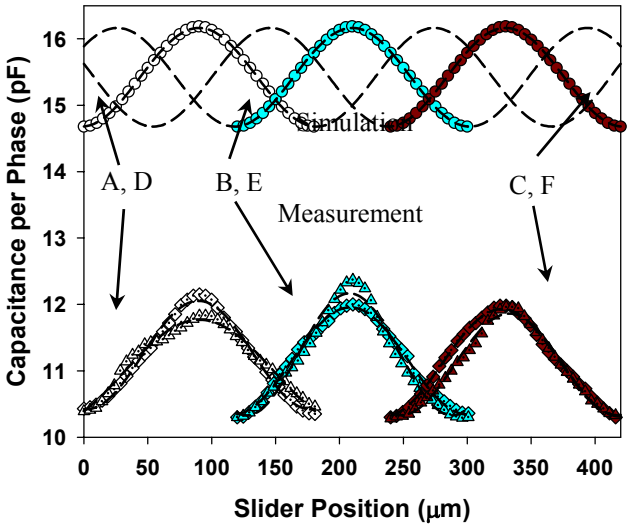

Figure 4. Simulated and measured capacitance of all B-LVCM six phases for device D2. The data is fit to sine-squared functions.

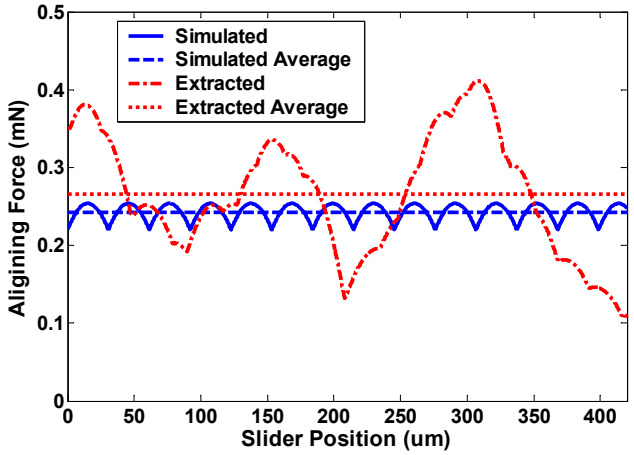

Figure 5. Simulated and extracted total aligning force and their average values. The force is calculated from curve fits to simulated and measured capacitance data of Figure 4.

their effect on the performance of the machine has been analyzed. The analysis is based on the governing equations for the speed, torque, mechanical, and electrical power of the micromachine.

The instantaneous electromechanical torque of the six-phase machine is given by

$$T(V,\theta) = \frac{1}{12} N_e V^2 \left(\frac{\partial C_1(\theta)}{\partial \theta} + \frac{\partial C_2(\theta)}{\partial \theta} + \frac{\partial C_3(\theta)}{\partial \theta} \right) \quad (3)$$

where *Ne* is the number of electrodes on the stator, *V* is the applied voltage, and $\partial C/\partial\theta$ is the derivative of the capacitance (of one electrode-pole pair) with respect to the angular position of the rotor (θ). Table 3 shows the average torque for two different designs with a 10-µm air gap and a

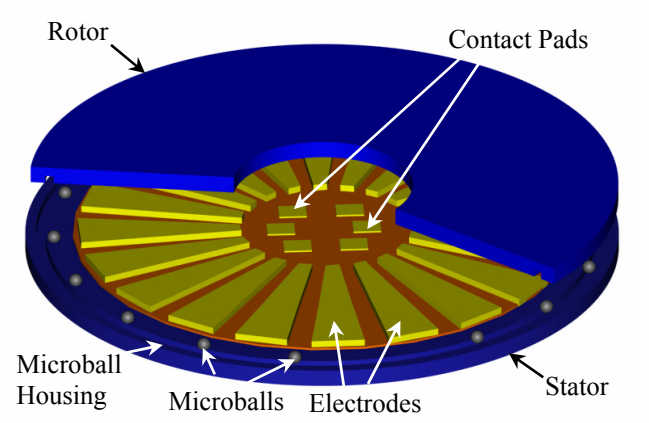

Figure 6. Schematic 3D view of the six-phase, bottom-drive, rotary, variable-capacitance micromachine.

Table 3. Two different designs for the B-RVCM.

	p/W	$\partial C/\partial\theta$ (pF/rad)	Synchronous speed (rpm) @ f_e=1 kHz	T_{ave} (μNm) @ V=100V
Design A	4/3	24.8	576.2	3.08
Design B	3/2	27.8	652.1	3.06

75-mm^2 active area. The electrode pitch-to-width ratio is different for each design. The torque is more than doubled if 5-μm air gap is achieved. Similarly, using FEA, the average lossless electrical power for the microgenerator, was calculated to be 181 μW at 60 krpm and with 10 V staring voltage (Design B). Simulations have shown that by decreasing the gap size from 10 μm to 5 μm, a lossless electrical power of 633 μW can be achieved for Design B.

6 CONCLUSION

We reported the design, fabrication, and characterization of a microball-bearing-supported bottom-drive linear variable-capacitance micromotor (B-LVCM) using benzocyclobutene polymer films as insulating layers. The successful development of the B-LVCM is the first demonstration of a MEMS device using microball bearing and BCB polymer technologies. The B-LVCM was fabricated based on the embedded benzocyclobutene in silicon (EBiS) process. The capacitance, aligning force, and slider speed were numerically calculated and experimentally measured. A comparison of the theoretical and experimental results showed that the B-LVCM operates as predicted with a deviation attributed to fabrication imperfections. An electromechanical model is being developed that can accurately predict the transient and steady-state operation of the device. The B-LVCM is used as a technology platform to design a microball-bearing-supported rotary micromotor/microgenerator.

ACKNOWLEDGEMENT

This work is supported by the National Science Foundation (NSF) under Grant No. ECS-0224361, the Army Research Office (ARO) through MAV MURI Program under Grant No. ARMY-W911NF0410176, with Technical Monitor as Dr. Gary Anderson, and the Army Research Lab (ARL) under CA# W911NF-05-2-0026. The authors would like to thank Nitta Haas Company, Japan for supplying the ILD1300 slurry. We would also like to thank Mr. Thomas C. Loughran and Mr. Nolan A. Ballew from University of Maryland, College Park, MD for help with fabrication.

REFRENCES

[1] A. Modafe, N. Ghalichechian, A. Frey, J. H. Lang, and R. Ghodssi, "A Microball-Bearing-Supported Linear Electrostatic Micromotor with Benzocyclobutene Polymer Insulating Layers," *Dig. Tech. Papers of the 13th Int. Conf. Solid-State Sensors, Actuators, and Microsystems (Transducers '05), Seoul, Korea*, pp. 693-696, 2005.

[2] R. Ghodssi, D. D. Denton, A. A. Seireg, and B. Howland, "Rolling friction in a linear microactuator," *Journal of Vacuum Science and Technology A*, vol. 11, pp. 803-807 (1993).

[3] M. E. Mills, P. Townsend, D. Castillo, S. Martin, and A. Achen, "Benzocyclobutene (DVS-BCB) Polymer as an Interlayer Dielectric (ILD) Material," *Microelectronic Engineering*, **33**, 327-334, 1997.

[4] T. –W. Lin, A. Modafe, B. Shapiro, and R. Ghodssi, "Characterization of Dynamic Friction in MEMS-Based Microball Bearings," *IEEE Trans. Instrumentation and Measurement*, **53** (3), 839-846, 2004.

[5] X. Tan, A. Modafe, R. Hergert, N. Ghalichechian, B. Shapiro, J. S. Baras, and R. Ghodssi, "Vision-based microtribological characterization of linear microball bearings," *ASME/STLE International Joint Tribology Conference (TRIB2004)*, Long Beach, CA, 2004.

[6] A. Modafe, N. Ghalichechian, and R. Ghodssi, "Electrical Characterization of Benzocyclobutene Polymers for Electric Micromachines," *IEEE Trans. Device and Materials Reliability*, vol. 4, pp. 495-508, 2004.

[7] N. Ghalichechian, A. Modafe, R. Ghodssi, P. Lazzeri, R. Micheli, M. Anderle, "Integration of Benzocyclobutene Polymers and Silicon Micromachined Structures Using Anisotropic Wet Etching," *J. Vac. Sci. Tech. (JVST) B*, vol. 22, pp. 2439-2447, 2004.

[8] A. Modafe, N. Ghalichechian, and R. Ghodssi, "Embedded Benzocyclobutene in Silicon (EBiS): An Integrated Fabrication Process for Electrical and Thermal Isolation in MEMS," *Microelectronic Engineering*, vol. 82, pp. 154-167, 2005.